JOURNAL OF NANO- AND ELECTRONIC PHYSICS
Vol. **8** No 4(2), 04078(4pp) (2016)
ЖУРНАЛ НАНО- ТА ЕЛЕКТРОННОЇ ФІЗИКИ
Том **8** № 4(2), 04078(4cc) (2016)

Photoelectrical and Gas-sensing Properties of Nanostructured ZnO/CuO Samples

A. Ogurcovs[1,*], Vj. Gerbreders[1], E. Tamanis[1], E. Sledevskis[1], A. Gerbreders[2]

[1] *Institute of Life Sciences and Technologies, Daugavpils University, P.O.5401 Daugavpils, Latvia*
[2] *Institute of Solid State Physics, University of Latvia, P.O.1063 Riga, Latvia*

(Received 18 October 2016; revised manuscript 19 December 2016; published online 23 December 2016)

An experimental *p-n* junction device was fabricated by synthesizing ZnO/CuO nanostructures via a hydrothermal process. The structural and optical properties of the ZnO/CuO nanocomposite were studied by X-ray diffraction (XRD), scanning electron microscope (SEM) and photovoltaic measurements. The XRD results showed the formation of the ZnO/CuO nanostructures (hexagonal wurtzite/monoclinic tenorite). The SEM images showed that the ZnO layer consists of vertically oriented nanorods and a CuO layer of nanosheets ranging in size from 1 to 1.5 um.The photovoltaic measurements indicated a certain level of photo-EMF. Vacuum tests revealed peculiar sensitivity to the atmospheric moisture of the ZnO/CuO samples.

Keywords: ZnO/CuO nanocomposite, Gas sensor, *p-n* junction, Photovoltaics, Hydrothermal synthesis.

DOI: 10.21272/jnep.8(4(2)).04078 PACS numbers: 81.07.Bc, 79.60.Jv.

1. INTRODUCTION

Zinc oxide (ZnO), an *n*-type metal oxide semiconductor with a wide band gap of 3.37 eV, has been widely investigated for many optoelectronic, gas sensor, solar cell and photocatalyst applications [1]. Copper oxide (CuO) is a p-type metal oxide semiconductor with a narrow band gap (1.2 eV). When the n-type semiconductor metal oxide is mixed with the p-type semiconductor metal oxide, it might be useful for new applications in material science [3, 4]. Among the semiconductor metal oxide nanocomposite materials, ZnO/CuO has attracted much attention and can be used for various applications such as optoelectronic devices, gas sensors and photocatalysts, etc. [5-7]. Composite nanomaterials can usually enhance certain functions in comparison with their individual components.

Basic function of gas sensors is converting sample gas concentration into electrical signal. Organic and inorganic matrials can be used as the gas-sensing materials [8]. Zinc oxide (metal oxide semiconductor of n-type conductivity) is used as a material for gas sensors [9] for several decades. Nanoscale semiconductor basd gas sensors has been widely studied in recent years. Size reduction to nanosclae of zinc oxide based gas sensors offers opportunities to significantly improve their sensing properties compared with macroscale counterparts. In order to improve commercially available gas sensors numerous attempts is undertaken to alter the sensing properties of metal oxide semiconductors [10], to increase their selectivity and sensitivity, faster response time and reduced operating temperature. Sensing properties of metal-oxide semiconductors can be improved by the use of nanostructures, such as nanoparticles, nanowires, nanorods et al. [11]. Quasi-one-dimensional metal-oxide nanostructures, such as nanowires and nanorods are more sensitive than volumetric materials for several reasons. Firstly, they have a higher ratio of volume and surface. This means that a significant part of such systems are surface atoms that can participate in the surface reaction. Secondly, the radius of nanowires is comparable to the shielding Debye length λ_D in a wide thermal range that causes a strong dependence of the electronic properties of the surface processes. Finally, the composition of the oxide semiconductor nanowires typically is closer to the stoichiometric, as they have higher degree of crystallinity compared to materials with granular structure [12]. Vertically oriented nanowires, unlike laterally oriented or cross-linked structures based on nanowires have additional useful properties. Since individual nanowires or bundles can be easily organized in vertical arrays, they are promising to scale devices, and creating integrated monolayer structures with maximum density [13-15]. Purpose of this work is to investigate sensor properties of hydrothermally grown ZnO/CuO nanocrystals forming the heterocontact interface on the nanoscale. Sensing properties of such structures are expected to be improved.

2. EXPERIMENT

On a glass substrate 250 nm thick ITO electrodes were deposited by means of magnetron sputtering with following annealing at 450 °C for 60 minutes (Fig. 1). Transparent ITO electrodes allowed the use of the photocell and gas sensor at the same time. For the directional growth of ZnO nanostructures, a Zn precursor layer was deposited on one of the electrodes by electrolysis in aqueous solution of Zn $(NO_3)_2$ at a molar concentration of 5.3 E – 3 mol/L. The metallic zinc layer obtained was annealed at 350 °C for 30 minutes in atmosphere. Growth of ZnO nanostructures was carried out with the hydrothermal method in an aqueous solution of Zn (NO3) 2 + C6H12N4 (HMT) at 75 °C for six hours. The same procedure was applied to the CuO on the second ITO electrode. Growth of CuO nanostructures was carried out in aqueous Cu (NO3) 2 + C6H12N4 (HMT) + NH3(25 %) at 75 °C for six hours. CuO growth solution is very active and it fills gaps be-

* andrejs.ogurcovs@gmail.com

tween ITO electrodes, ensuring electrical contact (Fig.1.d)). Unnecessary ITO areas were protected by a special mask. The devices were characterized by X-ray diffraction (Rigaku Smartlab) θ-2θ scan with CuKα (λ = 1.5405 A). Data analysis was done with Rigaku PDXL2 software.

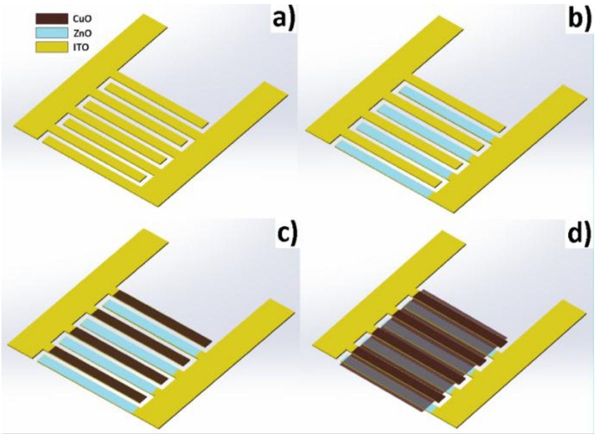

Fig. 1 – Schematic diagram of experimental sample structure and fabrication stages

The morphology of as-prepared samples was characterized by scanning electron microscopy (TESCAN VEGA LMU II). Solar measurements were done with an Oriel 2A solar light simulator coupled with a Picotest M3500A digital multimeter. Gas-sensing properties were measured with a Mantis deposition vacuum chamber coupled with the Picotest M3500A digital multimeter.

3. RESULTS AND DISCUSSION

SEM analysis of ZnO/CuO samples indicated a quite homogeneous surface of the ZnO layer consisting of more or less vertically oriented hexagonal ZnO nanocrystals (Fig. 2 a). The average ZnO nanocrystal is 1 um long and 150 nm wide and can be altered by changing growth conditions. Vertical orientation on nanocrystals is achieved by electrolytic deposition of a ZnO precursor. The main chemical reactions occurring during the growth process can be described according to:

$$C_6H_{12}N_4 + 6H_2O <> 4NH_3 + 6HCHO \quad (1)$$

$$NH_3 + H_2O <> NH_4^+ + OH^- \quad (2)$$

$$Zn^{2+} + 2OH^- <> Zn(OH) \quad (3)$$

Zn(OH)2 is a metastable compound that is dehydrolysed under the given conditions to produce ZnO according to:

$$Zn(OH)_2 <> ZnO + H_2O \quad (4)$$

All these reactions (1-4) are in equilibrium and can be controlled by adjusting parameters such as the source material concentration, the reaction temperature and the growth duration. The density of the grown nanorods is generally determined by the concentration of the reactants, and the reaction temperature and duration can be used to control the aspect ratio (length/diameter) [14]. Similar chemical reactions take place in CuO growth solution.

The CuO layer obtained is very homogeneous and its morphology is not affected by the structure of the bottom layer. CuO nanocrystals grow identically on

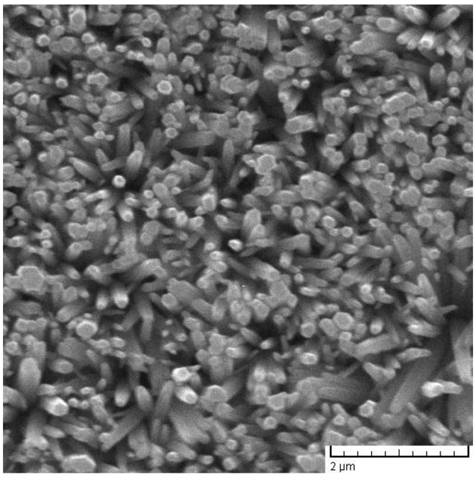

Fig. 2 – Hydrothermally grown ZnO nanostructures on ITO electrodes

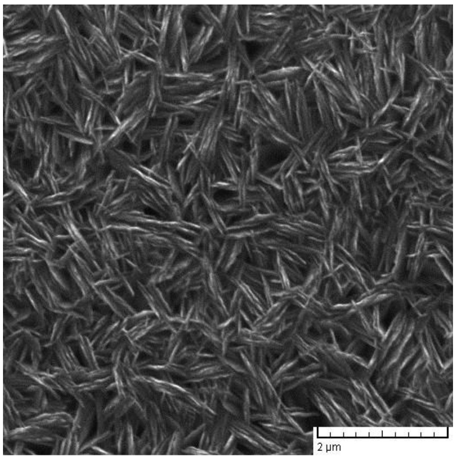

Fig. 3 – Hydrothermally synthesized cuo nanostructures on the top of ZnO layer

pure glass and on ZnO nanocrystals the only difference is in the mechanical properties of the film. Despite the same precursor deposition for the CuO layer, resulting CuO structures are 1 um long and 20 nm wide and chaotically oriented in the horizontal plane (Fig. 3).

XRD pattern analysis of ZnO/CuO samples revealed phase purity and good crystallinity of ZnO. The phase separation between ZnO and CuO is visible, confirming the existence of both ZnO and CuO. All peaks in XRD are in good agreement with the standard data (Fig. 4). More detailed analysis indicated the presence of a Cu_2O phase in an amount less than 1.8 % of the total cuo mass. In the xrd region from 20° to 40° can be observed a slightly amorphous background, probably related to the glass substrate of the sample.

During vacuum tests, the electrical response of the sample was measured with a computer-based system. The relative sensitivity was calculated according to:

$$S = (R_L - R_{air})/R_{air} \quad (5)$$

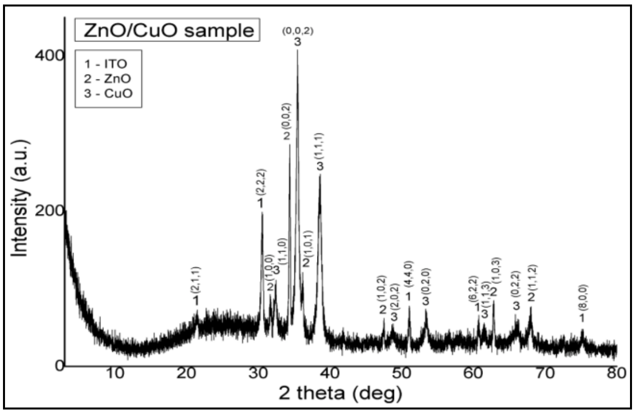

Fig. 4 – An xrd pattern of a hydrothermally grown ZnO/CuO sample

where S represents sensitivity, R_L resistance at low pressure, R_{air} resistance at normal pressure. Sample temperature was maintained at 25 °C. The test results presented in Fig.5 revealed interesting behaviour in terms of the resistance of samples. Sample sensitivity was $S = 62$ % in pressure ranging from 620 to 2.5 torr. The metal oxide gas sensor exhibited different sensitivity to various atmospheric gases and such resistance curves (Fig. 5) probably represented a superposition of sensitivity influenced by atmospheric moisture and complicated charge exchange in the p-n junction between the ZnO and CuO layers. The experimental sample is very sensitive to pressure changes although the reaction time is extremely high (Fig. 5, 6), presumably because of the huge surface area that slows down liberation of atmospheric gases from the surface of the test sample. Conductivity for resistive-type gas sensors is determined not by concentration of donor defects in the oxide structure, but by various forms of oxigen adsorption on the surface of crystal grains. The maximum of this effect is observed in nanocrystalline systems where surface role in electrical properties of materials is most significant [18].

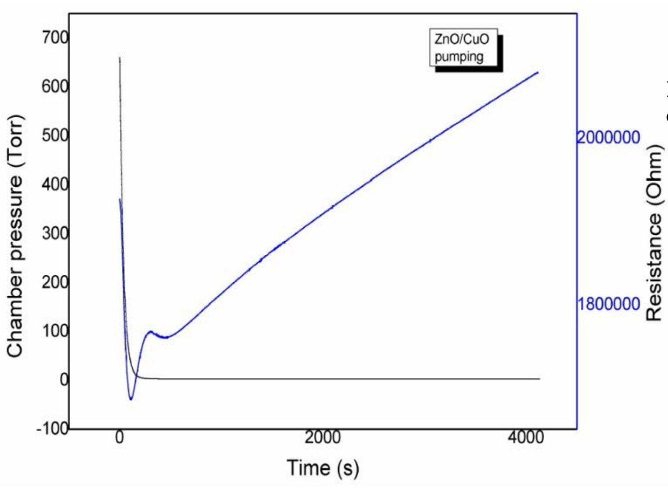

Fig. 5 – Changes in resistance of ZnO/CuO sample during decreasing atmospheric pressure (pumping)

Hysteresis loop in humidity sensors can be explained by the Kelvin effect, that delays or prevents the desorption of water that condenses in the ZnO pores during adsorption, forming a meniscous. One way to

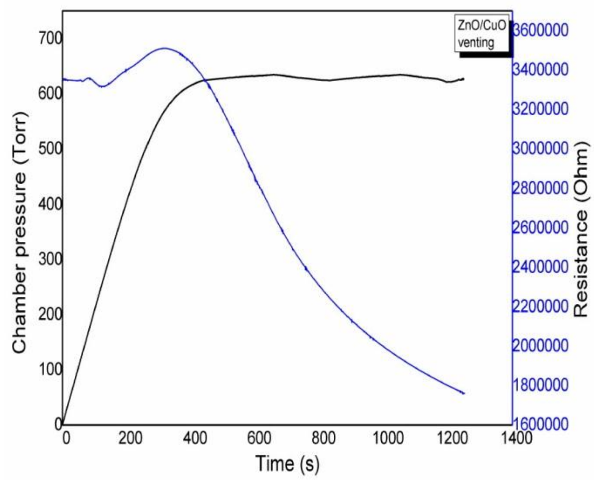

Fig. 6 – Changes in resistance of ZnO/CuO sample rising pressure (venting)

solve this problem is to increase working temperature, that will accelerate the desorption of water and hydroxyl groups. Analysis led to the conclusion that resistance of ZnO/CuO films depends not only on the relative humidity, but the way it changes, that can lead to difficulties in usage of such structures as a gas sensors at room temperature [18].

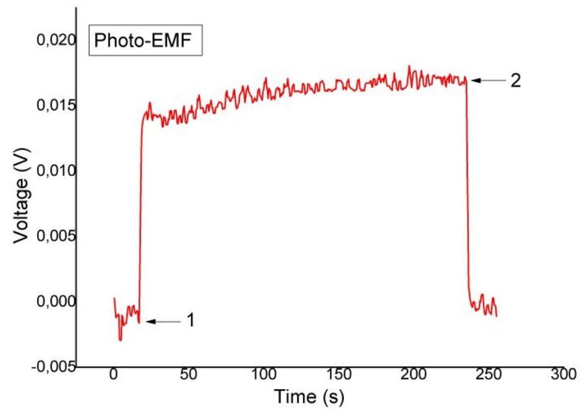

Fig. 7 – Photo-emf response to artificial solar radiation level of the ZnO/CuO sample

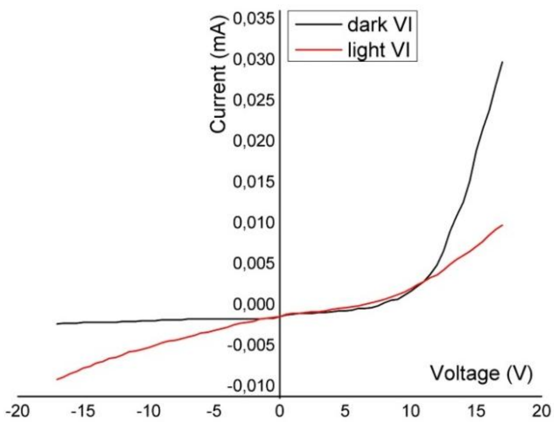

Fig. 8 – VI curves in darkness and during illumination

During exposure to artificial solar radiation, samples generated a photo-emf level of $U_{ph} = 16.5E-3$ V. An immediate reaction to the start of exposure was observed (Fig. 7 Photo-EMF), point 1) and same reaction to the end of exposition (Fig. 7. point 2). EMF level is quite noisy, probably because of the thermal drift of charge carriers in the ZnO/CuO contact zone. However, VI curve measurements indicated almost complete degradation of potential barriers in the ZnO/CuO contact region (Fig. 8 light VI). The observed effect might be a result of a decrease in the height of the potential barrier caused by the generation of electrically active point defects, with both donor and acceptor levels created. If the generated defects are the charge carrier recombination centres, this will lead to a decrease in the photo-emf level.

4. CONCLUSION

Hydrothermally grown ZnO/CuO samples exhibit high sensitivity to atmospheric gases due to high surface area, however reaction time is rather high. The presence of p-n junction in the ZnO/CuO contact region makes possible to use such samples as a light sensors and and presumably, adjust the sensitivity of samples to atmospheric gases by applying bias potential. However application in photovoltaics is limited because of residual tension and defects in the crystalline lattices of the materials, which causes the appearance of parasitic charge and recombination centres. Described method and materials has potential for use in production because of its cheapness and simplicity.

ACKNOWLEDGEMENTS

This study was supported by ESF project Nr.2013/0029/1DP/1.1.1.2/13/APIA/VIAA/029.

REFERENCES

1. J. Huang, Z. Yin, Q. Zheng, *Energy Environ. Sci.* **4**, 3861 (2011).
2. H. Kidowaki, T. Oku, T. Akiyama, A. Suzuki, B. Jeyadevan, J. Cuya, *J. Mat. Sci. Res.* **1**, 138 (2012).
3. B. Li , Y. Wang, *Superlattice. Microst.* **47**, 615 (2010).
4. R. Saravanan, S. Karthikeyan, V.K. Gupta, G. Sekaran, V. Narayanan, A. Stephen, *Mat. Sci. Eng. C.* **33**, 91 (2013).
5. M.S. Spencer, *Top. Catal.* **8**, 259 (1999).
6. A.B. Djurišić, A.M.C. Ng, X.Y. Chen, *Prog. Quant. Electron.* **34**, 191 (2010).
7. L. Perazolli, L. Nunez, M.R. Apolinario da Silva, G. Francisco, P. Ademir, G. Cavalarri Costalonga, R. Gimenes, M.M. Kondo, M.A.Z. Bertochi, *Mat. Sci. Appl.* **2**, 564 (2011).
8. A.S. Komolov, P.J. Moller, J. Mortensen, S.A. Komolov, E.F. Lazneva, *Surf. Sci.* **586**, 129 (2005).
9. Ed. M.A. Carpenter, S. Mathur, A. Kolmakov. *NY: Springer Science + Business Media*, **548** (2013).
10. M.S. Spencer, *Top. Catal.* **8**, 259 (1999).
11. A.B. Djurišić, A.M.C. Ng, X.Y. Chen, *Prog. Quant. Electron.* **34**, 191 (2010).
12. Y.H. Ko, S.H. Lee, J.S. Yu, *SPIE Newsroom* (2014)
13. F.Z. Haque, N. Singh, P. Ranjan, *Int. J. Sci. Eng. Res.* **5**, 149 (2014)
14. Z. Guo, X. Chen, J. Li, J.H. Liu, X.J. Huang, *Langmuir* **27**, 6193 (2011).
15. Q. Simon, D. Barreca, A. Gasparotto, C. Maccato, E. Tondello, C. Sada, E. Comini, G. Sberveglieri, M. Banerjee, K. Xu, A. Devi, R.A. Fischer, *Chemphyschem* **13** (2012)
16. A. Eltahir, E. Zainelabdin, *Linkoping Studies in Science and Technology Dissertation*, 1484 (2012).
17. Ch. Wang, L. Yin, L. Zhang, D. Xiang, R. Gao, *Sensors* **10**, 2088 (2010).
18. T.V. Peshkova, D.Ts. Dimitrov, S.S. Nalimova, I.E. Kononova, N.K. Nikolaev, K.I. Kapazova, A.S. Bozhinova, V.A. Moshnikov, E.I. Terukov, *Tech. Phys.* **59** No 5, 771 (2014).